A Comparison of the Element Free Galerkin Method and the Meshless Local Petrov-Galerkin Method for Solving Electromagnetic Problems

Wei He [1], Zehui Liu [1], Richard K. Gordon[2], W. Elliott Hutchcraft[2], Fan Yang[1] and Afei Chang[3]

[1] School of Electrical Engineering
Chongqing University, Chongqing, 400044, China
hewei@cqu.edu.cn, lzhking2000@gmail.com, yangfancqu@gmail.com

[2] Department of Electrical Engineering
University of Mississippi, University, MS 38677, USA
eegordon@olemiss.edu, eeweh@olemiss.edu

[3]State Nuclear Electric Power Planning Design & Research Institute
Beijing, 100095, China
yafei0205@126.com

Abstract ─ In this paper, the element free Galerkin (EFG) method and the local Petrov-Galerkin (MLPG) method are compared for solving the electromagnetic problems. The EFG method and MLPG method are introduced at first. Both of the EFG and the MLPG methods are formulated in detail with Poisson's equation. Based on basic electromagnetic problems, the numerical results from the EFG method and MLPG method are given in this paper. The numerical results show that the EFG method and MLPG method both work well for the solution of electromagnetic problems. The EFG method, based on global weak form, needs background meshes for integration, and it needs more nodes to get an accurate result but it requires less cost in computational time. The MLPG method as a true meshless method doesn't needs any meshes in the implementation and can obtain an accurate result using fewer nodes than EFG. However, because the MLPG Method needs more integration nodes and has asymmetric matrices, it needs more CPU time than the EFG method with the condition that the same number of nodes is used in the problem domain.

Index Terms ─ electromagnetic problems, meshless method, the element free Galerkin method, the local Petrov-Galerkin method.

I. INTRODUCTION

With the development of the computational technologies, the modeling and simulation of engineering problems can be solved by the numerical methods. For decades, people have been using the finite-element method (FEM), boundary-element method (BEM) and finite-difference method (FDM) to solve the partial differential equation of the engineering systems [1]. Among those methods, the finite-element method is mostly widely used to solve the more-challenging problems as they require increasing demands on flexibility, effectiveness and accuracy for challenging problems with complex geometry [2]. However, the FEM requires the solution domain to be meshed, and the accuracy of the FEM depends on the quality of the mesh [1], and the mesh generation is more time consuming and a more expensive task than the solution of the finite element equations [3]. A lot of efforts have made to improve the design mesh, but it is still a challenge for some engineering analyses such as

Submitted On: Feb. 29, 2012
Accepted On: June 24, 2012

the dimensionally very small air gaps and the remaining electromagnetic structures.

To avoid these problems, recently a class of new methods called meshless or meshfree methods have been developed. The meshless methods do not require the generation of a mesh of the solution domain. The only necessary information are sets of nodes scattered in the solution domain as well as sets of nodes scattered on the boundaries, which means no mesh generation at the beginning of the calculation is needed.

There are many different types of meshless methods [4-8], some important examples of these methods include the smooth particle hydrodynamics (SPH) method, the diffuse-element method (DEM), the reproducing kernel particle method (RKPM), the element-free Galerkin (EFG) method, the meshless local Petrov-Galerkin (MLPG) method, the local boundary integral equation (LBIE) method, the hp-cloud method, the finite point method (FPM), and so on.

In those methods, the element free Galerkin (EFG) method (Belytschko et al., 1992) is one of the most viable methods and has become an inspiration source for the latter meshless methods. EFG method is based on the global weak-forms, so it requires background cells for evaluation of the integrals of the weak-forms. The meshless local Petrov-Galerkin (MLPG) method (Atluri and Zhu et al, 1998) is based on the local symmetric weak form (LSWF). The MLPG Method does not need elements or meshes either for interpolation purposes or for integration purposes. All integrals in the MLPG Method are carried out only on spheres (in 3-D or circles in 2-D) centered at each point in question [3,9,10]. Based on different type combinations of trial and test functions, there are six different schemes of the MLPG method [11].

Both the EFG method and the MLPG1 method are based on the moving least squares (MLS) approximation for the construction of the meshless shape functions. There are two differences between the EFG method and the MLPG method [12]. In the first place, the trial and test function in EFG are taken from the same functional spaces while they can be different for the MLPG method. Second, the main difference of them is the weak form used. The EFG method uses the global weak form and needs the background cells for the integration, but the MLPG method is based on the local symmetric weak form, so it does not need the background cells and thus is a truly meshless method.

In this paper, the EFG method and the MLPG method are formulated in detail and a comparison is made in their solution of an electromagnetic problem. The numerical results show that EFG method and MLPG method both work well for the electromagnetic problem. The EFG method needs more nodes to get an accurate result but has the advantage that the computation time is lower. The MLPG method doesn't need any background meshes in its implementation and can obtain an accurate result using fewer nodes than EFG, but the MLPG method requires more CPU time.

The following discussion begins with the brief description of the moving least squares (MLS) approximation which is used to construct the shape function for both the EFG method and the MLPG method in Section Ⅱ.The basic numerical implementation of EFG method and MLPG method are given in Section Ⅲ. The numerical examples are given in Section Ⅳ. The paper ends with conclusions and discussions in Section Ⅴ.

II.THE MOVING LEAST SQUARES APPROXIMATION

The MLS method was first introduced by Lancaster and Salkauskas [13]. The MLS has main two major features: (1) the approximated field function is continuous and smooth in the entire problem domain; (2) the MLS method can produce an approximation with the desired order of consistency [2]. Those two features make the MLS method the most widely used method for the construction of the meshless shape functions.

A. The MLS approximation scheme

Consider $u(x)$ to be the function of the field variable defined in the problem domain Ω. The approximation of $u(x)$ is denoted $u^h(\mathbf{x})$:

$$u^h(\mathbf{x}) = \sum_j^m p_j(\mathbf{x}) a_j(\mathbf{x}) \equiv \mathbf{p}^T(\mathbf{x})\mathbf{a}(\mathbf{x}), \quad (1)$$

where m is the number of terms of monomials (polynomial basis), and $\mathbf{a(x)}$ is a vector of coefficients given by

$$\mathbf{a}^T(x) = \{a_0(x)\ a_1(x)\ \ldots\ a_m(x)\}, \quad (2)$$

which are functions of x.

In equation (1), $\mathbf{p}(\mathbf{x})$ is a vector of complete

monomial basis; m is the number of the terms in the basis. In this paper, the linear basis is used for 1D and 2D:

$$\mathbf{p}^T(\mathbf{x}) = [1 \;\; x], \quad in\ 1D, \tag{3}$$

$$\mathbf{p}^T(\mathbf{x}) = [1 \;\; x \;\; y], \quad in\ 2D. \tag{4}$$

The linear basis assures the MLS approximation has the linear completeness and can reproduce any smooth function and its first derivative with arbitrary accuracy [11]. The coefficients $a_j(\boldsymbol{x})$ can be obtained at the point $\mathbf{x}$ by minimizing a weighted discrete L_2 norm as follows:

$$J = \sum_{I=1}^{n} w(\mathbf{x}-\mathbf{x}_I)[\mathbf{p}^T(\mathbf{x}_I)\mathbf{a}(\mathbf{x}) - u_I]^2, \tag{5}$$

where n is the number of nodes in the neighborhood of $\mathbf{x}$ which weight function $w(\mathbf{x}-\mathbf{x}^I) \geq 0$. The u_I is the value of u at $\mathbf{x}=\mathbf{x}_I$. The neighborhood of $\mathbf{x}$ size is called the domain of influence of $\mathbf{x}$.

To obtain $\boldsymbol{a}(\boldsymbol{x})$ at an arbitrary point $\mathbf{x}$, the minimization condition is required:

$$\frac{\partial J}{\partial \mathbf{a}} = 0, \tag{6}$$

which leads to the following linear equation system:

$$\mathbf{A}(\mathbf{x})\mathbf{a}(\mathbf{x}) = \mathbf{B}(\mathbf{x})\mathbf{U}_s, \tag{7}$$

where the matrices $\mathbf{A}(\mathbf{x})$, $\mathbf{B}(\mathbf{x})$ and $\mathbf{U}_s$ are defined by

$$\mathbf{A}(\mathbf{x}) = \sum_{I}^{n} w(\mathbf{x}-\mathbf{x}_I)\mathbf{p}^T(\mathbf{x}_I)\mathbf{p}(\mathbf{x}_I), \tag{8}$$

$$\mathbf{B}(\mathbf{x}) = [w_1(\mathbf{x}-\mathbf{x}_1)\mathbf{p}(\mathbf{x}_1),\ w_2(\mathbf{x}-\mathbf{x}_2)\mathbf{p}(\mathbf{x}_2), \ldots, w_n(\mathbf{x}-\mathbf{x}_n)\mathbf{p}(\mathbf{x}_n)], \tag{9}$$

$$\mathbf{U}_s = [U_1, \;\; U_2, \ldots, U_n]. \tag{10}$$

Solving the equation (7) for $\mathbf{a}(\mathbf{x})$ we obtain:

$$\mathbf{a}(\mathbf{x}) = \mathbf{A}^{-1}(\mathbf{x})\mathbf{B}(\mathbf{x})\mathbf{U}_s. \tag{11}$$

Hence, we have:

$$u^h(\mathbf{x}) = \sum_{I}^{n}\sum_{j}^{m} p_j(\mathbf{x})(\mathbf{A}^{-1}(\mathbf{x})\mathbf{B}(\mathbf{x}))_{jI} u_I \equiv \sum_{I}^{n} \Phi_I(\mathbf{x}) u_I, \tag{12}$$

where the shape function is defined by:

$$\Phi_I(\mathbf{x}) = \sum_{j}^{m} p_j(\mathbf{x})(\mathbf{A}^{-1}(\mathbf{x})\mathbf{B}(\mathbf{x}))_{jI}. \tag{13}$$

The partial derivatives of $\Phi_I(\mathbf{x})$ can be obtained [3]:

$$\Phi_{I,i} = \sum_{j}^{m} \left\{ p_{j,i}(\mathbf{A}^{-1}\mathbf{B})_{jI} + p_j(\mathbf{A}_{,i}^{-1}\mathbf{B} + \mathbf{A}^{-1}\mathbf{B}_{,i})_{jI} \right\}, \tag{14}$$

where: $\mathbf{A}_{,i}^{-1} = -\mathbf{A}^{-1}\mathbf{A}_{,i}\mathbf{A}^{-1}$ and $(\;)_{,i}$ denotes $\partial(\;)/\partial x^i$.

B. Choice of weight function

There are many types of weight functions that can be chosen [2]. The following weight function is adopted in this paper [14]:

$$w(\mathbf{x}-\mathbf{x}_I) \equiv w(r) = \begin{cases} \frac{2}{3} - 4r^2 + 4r^3 & for\ r \leq \frac{1}{2} \\ \frac{4}{3} - 4r + 4r^2 - \frac{4}{3}r^3 & for\ \frac{1}{2} < r \leq 1 \\ 0 & for\ r > 1 \end{cases}, \tag{15}$$

where $r = d_I / d_{mI}$, $d_I = \|\mathbf{x}-\mathbf{x}_I\|$ and d_{mI} is the size of the domain of influence of the I^{th} node.

III. IMPLEMENTATION OF THE EFG METHOD AND THE MLPG METHOD

In this section, a basic domain obeying Poisson's equation function and boundary conditions is considered to demonstrate the formulation of the EFG method and the MLPG method. The governing equation and boundary conditions are expressed as:

$$\nabla^2 u(\mathbf{x}) = -\frac{\rho(\mathbf{x})}{\varepsilon} \quad \mathbf{x} \in \Omega. \tag{16}$$

The essential and the natural boundary conditions are respectively given by:

$$u(\mathbf{x}) = u_0 \quad on\ \ \Gamma_u, \tag{17a}$$

$$\frac{\partial u(\mathbf{x})}{\partial \mathbf{n}} \equiv q = \bar{q} \quad on\ \ \Gamma_q, \tag{17b}$$

where the domain is enclosed by $\partial\Omega = \Gamma_u \cup \Gamma_q$ and $\mathbf{n}$ is the outward normal direction to the boundary.

A. The EFG method formulation

The EFG method is based on the globe weak form on the global problem domain Ω and the essential boundary conditions can be imposed by the penalty method by penalty parameter. The equivalent weak form of Poisson's function is:

$$\int_{\Omega}\left(\nabla^2 u + \frac{\rho(\mathbf{x})}{\varepsilon}\right) v d\Omega - \alpha\int_{\Gamma_u}(u-u_0)v d\Gamma = 0, \tag{18}$$

where u is the trial function approximated by the MLS method, v is the test function, and $\alpha >> 1$ is a penalty parameter used to impose the essential boundary conditions.

Using the formula $\left(\nabla^2 u\right)v = u_{,ii}v = \left(u_{,i}v\right)_{,i} - u_{,i}v_{,i}$, the divergence theorem and $u_{,i}ni = \partial u / \partial n \equiv q$, we can derive the local weak form as:

$$\int_\Omega \left(\nabla v \cdot \nabla u - \frac{\rho(\mathbf{x})}{\varepsilon} v \right) d\Omega - \int_{\partial\Omega} qv d\Gamma + \alpha \int_{\Gamma_u} (u - u_0) v d\Gamma = 0. \quad (19)$$

Imposing the natural boundary (17b), we can obtain:

$$\int_\Omega (\nabla v \cdot \nabla u) d\Omega + \alpha \int_{\Gamma_u} uv d\Gamma - \int_{\Gamma_u} qv d\Gamma = \int_{\Gamma_q} \bar{q} v d\Gamma + \alpha \int_{\Gamma_u} u_0 v d\Gamma + \int_\Omega \frac{\rho(\mathbf{x})}{\varepsilon} v d\Omega. \quad (20)$$

When the trial functions and test functions are taken from the same function space and produced by Eq. (12) [3], we can discretize Eq. (20) as:

$$\mathbf{Ku} = \mathbf{f}, \quad (21)$$

where the matrix $\mathbf{K}$ and the vector $\mathbf{f}$ are define by:

$$K_{ij} = \int_\Omega \nabla \Phi_i \cdot \nabla \Phi_j d\Omega + \alpha \int_{\Gamma_u} \Phi_i \Phi_j d\Gamma - \int_{\Gamma_u} \Phi_i \frac{\partial \Phi_j}{\partial \mathbf{n}} d\Gamma. \quad (22)$$

$$f_i = \int_{\Gamma_q} \bar{q} \Phi_i d\Gamma + \alpha \int_{\Gamma_u} \bar{u} \Phi_i d\Gamma + \int_{\Omega_s} \frac{\rho(\mathbf{x})}{\varepsilon} \Phi_i d\Omega. \quad (23)$$

B. The MLPG method formulation

The MLPG method is based on the local symmetric weak form over a local sub-domain Ω_s, the local sub-domain Ω_s is entirely inside the global problem domain Ω. A local weak form of the governing equation (16) and the boundary conditions (17) can be written as:

$$\int_{\Omega_s} \left(\nabla^2 u + \frac{\rho(\mathbf{x})}{\varepsilon} \right) v d\Omega - \alpha \int_{\Gamma_{su}} (u - u_0) v d\Gamma = 0, \quad (24)$$

where u, v and $\alpha >> 1$ are the trial functions, test functions and penalty parameter respectively. Γ_{su} is a part of the essential boundary Γ_u. If the sub-domain has no intersection with the global essential boundary Γ_u, the second part of equation (24) vanishes [11].

Corresponding to the EFG formulation, the local weak form can be written as:

$$\int_{\Omega_s} \left(\nabla v \cdot \nabla u - \frac{\rho(\mathbf{x})}{\varepsilon} v \right) d\Omega - \int_{\partial\Omega_s} qv d\Gamma + \alpha \int_{\Gamma_{su}} (u - u_0) v d\Gamma = 0. \quad (25)$$

Using the natural boundary condition (17b) we can obtain:

$$\int_{\Omega_s} \left(\nabla v \cdot \nabla u - \frac{\rho(\mathbf{x})}{\varepsilon} \right) v d\Omega - \int_{L_s} qv d\Gamma - \int_{\Gamma_{su}} qv d\Gamma - \int_{\Gamma_{sq}} \bar{q} v d\Gamma + \alpha \int_{\Gamma_{su}} (u - u_0) v d\Gamma = 0. \quad (26)$$

where Γ_{sq} is a part of the natural boundary of Γ_q, if a sub-domain is totally inside the globe domain and has no intersection between Ω_s, the $L_s = \partial\Omega_s$ and the integrals over Γ_{su} and Γ_{sq} vanish [11].

The weight function used in the MLS approximation is chosen as the test function in the MLPG method. So the test function will vanish on the boundary of the local domain Ω_s and the boundary L_s. Using this function, the function (26) can be rewritten as:

$$\int_{\Omega_s} \nabla w_s \cdot \nabla u d\Omega + \alpha \int_{\Gamma_{su}} w_s u d\Gamma - \int_{\Gamma_{su}} w_s q d\Gamma = \int_{\Gamma_{sq}} w_s \bar{q} d\Gamma + \alpha \int_{\Gamma_{su}} w_s \bar{u} d\Gamma + \int_{\Omega_s} w_s \frac{\rho(\mathbf{x})}{\varepsilon} d\Omega. \quad (27)$$

To obtain the discrete equations, substitution of (12) into (27), we can discretize Eq. (27) as:

$$\mathbf{Ku} = \mathbf{f}, \quad (28)$$

where

$$K_{ij} = \int_{\Omega_s} \nabla w_s \cdot \nabla \Phi_j d\Omega + \alpha \int_{\Gamma_{su}} w_s \Phi_j d\Gamma - \int_{\Gamma_{su}} w_s \frac{\partial \Phi_j}{\partial \mathbf{n}} d\Gamma, \quad (29a)$$

and

$$f_i = \int_{\Gamma_{sq}} w_s \bar{q} d\Gamma + \alpha \int_{\Gamma_{su}} w_s \bar{u} d\Gamma + \int_{\Omega_s} w_s \frac{\rho(\mathbf{x})}{\varepsilon} d\Omega. \quad (29b)$$

IV. NUMERICAL EXPERIMENTS

In this paper, the essential boundary conditions in the EFG and MLPG methods are both imposed by the penalty method with the penalty parameter α being chosen as 10^6 [2,12]. The number of integration points is chosen to be three times the total number of nodes in EFG, the local quadrature domain Ω_s with four subdivision cells and 4×4 integration points in each cell is used in the local quadrature domain in MLPG method [3].

In order to investigate the accuracy of the EFG and MLPG methods, a relative error is calculated as follows [12]:

$$Error = \frac{\max_{1\le i\le N}\left\|u_i^{num}-u_i^{ana}\right\|}{\max_{1\le i\le N}u_i^{ana}}, \qquad (30)$$

where u_i^{num} denotes the numerical solution of the ith node and the u_i^{ana} denotes the analytic solution of the ith node.

A. Solution of Poisson's equation

We first consider Poisson's equation with the problem domain illustrated in Fig. 1. As shown in Fig. 1, the size of the problem domain is $\Omega \equiv (0,10)\times(0,10)$ with dielectric constant ε_0. The governing equation and boundary condition are as follows:

$$\nabla^2 u(\mathbf{x}) = -\pi^2\left(\frac{1}{a_1^2}+\frac{1}{a_2^2}\right)\sin\left(\frac{y}{a_1}\pi\right)\cos\left(\frac{x}{a_2}\pi\right)\frac{\rho_0}{\varepsilon_0}, \qquad (31)$$

$$u(\mathbf{x}) = 0 \quad on\ \ \Gamma_u, \qquad (32a)$$

$$\frac{\partial u(\mathbf{x})}{\partial \mathbf{n}} = 0 \quad on\ \ \Gamma_q. \qquad (32b)$$

where ρ_0 is the distribution density, $\rho_0 = -100C/m^2$, ε_0 is dielectric constant and two choices of a_1 and a_2 have been made such that $a_1, a_2 \in \{1, 2, 5, 10\}$.

With different a_1 and a_2 the analytic solution is different. The analytic solution of this problem is:

$$u(\mathbf{x}) = \sin\left(\frac{y}{a_1}\pi\right)\cos\left(\frac{x}{a_2}\pi\right)\frac{\rho_0}{\varepsilon_0}. \qquad (33)$$

The Analytical solution based on equation (33) is shown in Figs. 2 and 3 for different values of a_1 and a_2. A comparison of the exact solution with numerical results from both EFG and MLPG methods along the line x=5 is shown in Fig. 4 and Fig. 5. The total number of nodes was 400 for Fig. 4 and 2500 nodes for Fig. 5. Each Fig shows the results for the two different values of a_1 and a_2.

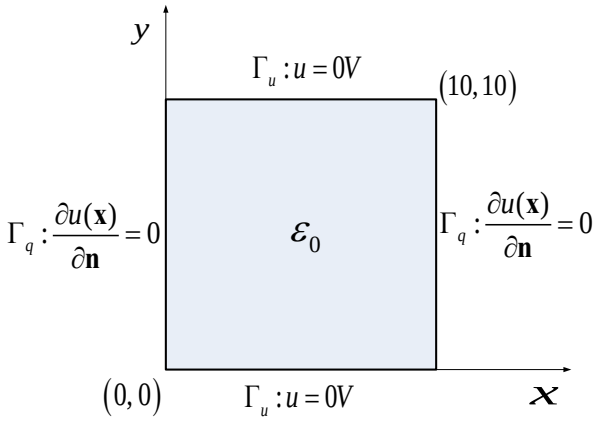

Fig. 1. Problem domain for Poisson's equation.

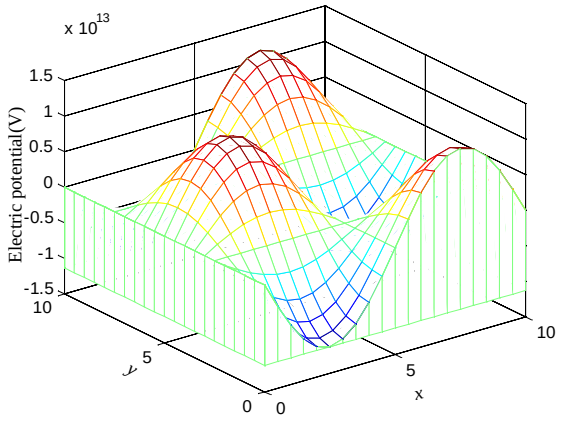

Fig. 2. The analytic solution of the Poisson's problem with a_1=5 and a_2=5.

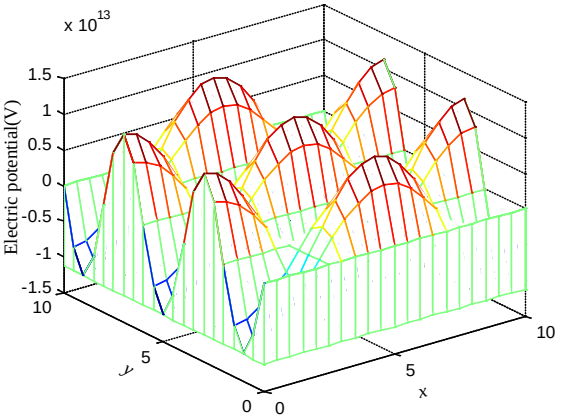

Fig. 3. The analytic solution of the Poisson's problem with a_1=2 and a_2=5.

We can observe good agreement between analytical and numerical results from Fig. 4 and Fig. 5. And the numerical results become more accurate as more nodes are used in the calculation.

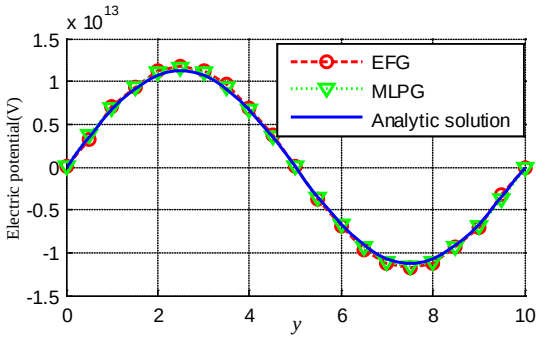

(a) a_1=5 and a_2=5.

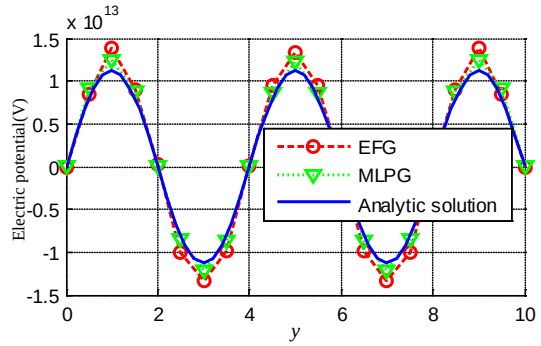

(b) a_1=2 and a_2=5.

Fig. 4. Comparison between the analytic solution, EFG method and MLPG method with 400 nodes along x=5 .

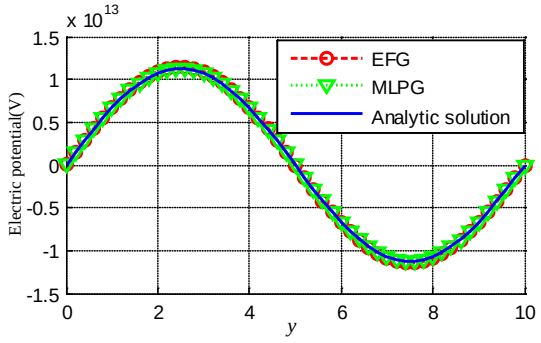

(a) a_1=5 and a_2=5.

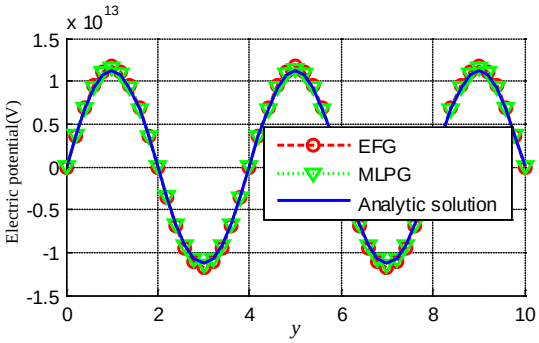

(b) a_1=2and a_2=5.

Fig. 5. Comparison between the analytic solution, EFG and MLPG method with 2500 nodes used along x=5.

B. Solution of Helmholtz equation

Next, let us consider a problem domain which is governed by the Helmholtz equation [8]:

$$\nabla^2 E_z + k^2 E_z = 0 \quad for\ (x,y) \in \Omega, \tag{34}$$

$$E_z(x,y) = f(x,y) \quad for\ (x,y) \in \partial\Omega. \tag{35}$$

The problem domain along with the associated boundary conditions is illustrated in Fig. 6.

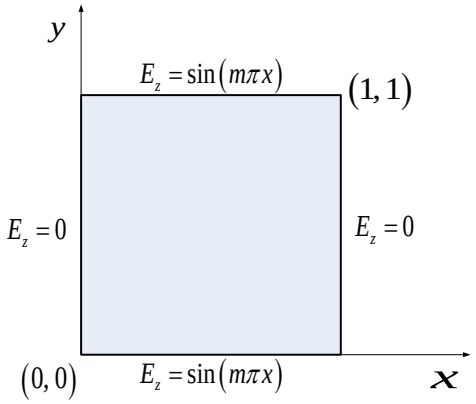

Fig. 6. Example of Helmholtz equation.

Consider the case for which $\lambda = \dfrac{2\pi}{k} = 1$. The analytic solutions of this problem with two different choices of m in boundary conditions are shown in Figs. 7 and 8.

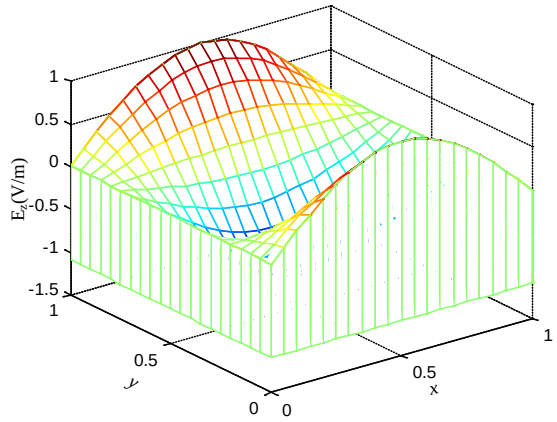

Fig. 7. The analytic solution of the Helmholtz equation with m=1.

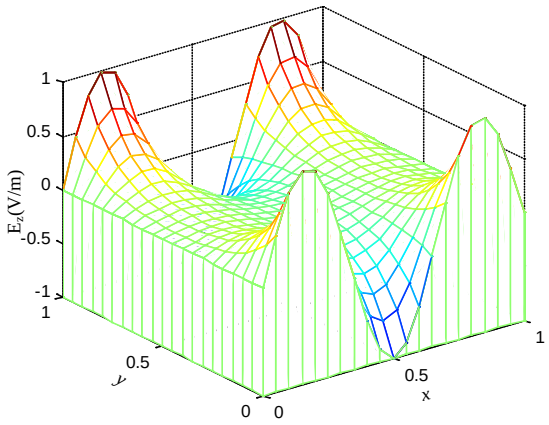

Fig. 8. The analytic solution of the Helmholtz equation with m=3.

A comparison of the exact solution with numerical results from both EFG and MLPG methods along the line y=0.5 is shown in Fig. 9 and Fig. 10. The total number of nodes was 400 for Fig. 9 and 2500 nodes for Fig. 10.

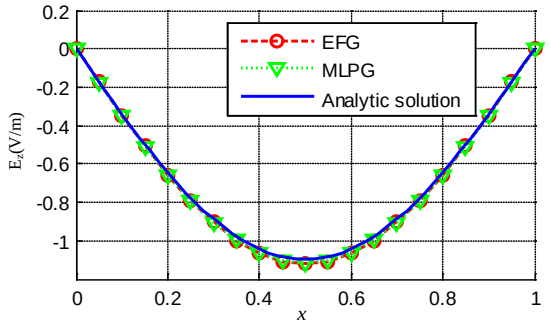

(a) The analytic and numerical solutions with m=1.

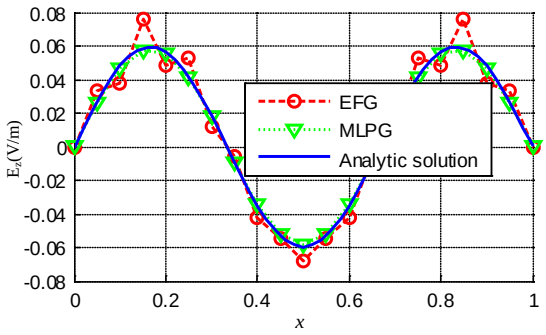

(b) The analytic and numerical solutions with m=3.

Fig. 9. Comparison between the analytic solution, EFG method and MLPG method with 400 nodes along y=0.5.

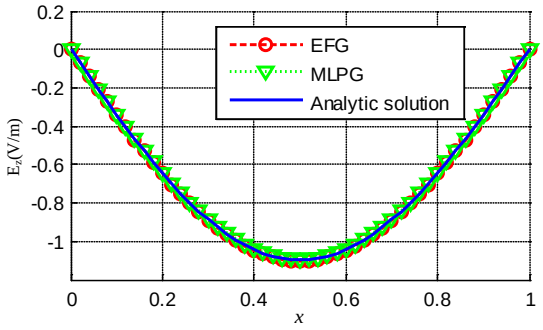

(a) The analytic and numerical solutions with m=1.

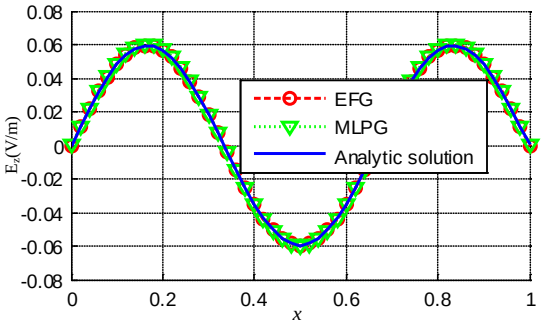

(b) The analytic and numerical solutions with m=3.

Fig. 10. Comparison between the analytic solution, EFG method and MLPG method with 2500 nodes along y=0.5.

According to the results shown in Fig. 9 and Fig. 10, it can be concluded that both the EFG method and MLPG method work well for the Helmholtz problem. In addition, more nodes used

in the model, more accurate of the results, this is the same as that in the example of Poisson's problem.

Based on the analytic solutions with different a_1 and a_2 in Poisson's problem, the relative error and computational efficiency of EFG and MLPG method are investigated.

In order to discuss the relationship of the relative error, the total number of nodes with different problems (different a_1 and a_2), a relative error with different number of nodes in EFG method and MLPG method is given in Fig. 11. Figure 11 shows the MLPG method is more accurate than EFG with the same number of nodes, especially when the total number of nodes is substantially lower. With the increase of total number of nodes used, the relative error of both EFG method and MLPG method are getting close to zero.

For the case where a_1=2 and a_2=5, the analytic electric potential is much more complex than the case where a_1=a_2=5, more nodes are required to get an exact answer.

To investigate the computational efficiency of the two methods, the average processing time required as a function of the total number of nodes is obtained and plotted in Fig. 12. It should be noted that he computation was done with the same Lenovo computer.

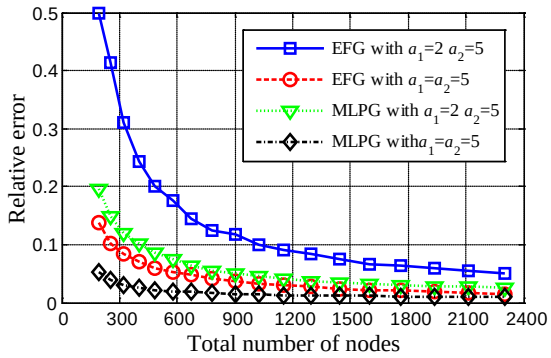

Fig. 11. Relative error with the total number of nodes in EFG and MLPG method.

It can be found that, the MLPG method needs more processing time than the EFG method. It is mainly due to the following two reasons: At first, the MLPG method requires more integration points than the EFG method in the computation. Both of the EFG method and the MLPG method need to integrate over the domain. The EFG method needs shadow meshes to set integration points over the entire domain of the problem. The MLPG method doesn't need elements or meshes for integration, all the integrals are carried out on spheres centered at each node in the domain, so the MLPG method can be referred to as a "real" meshless method or at least close to the ideal mesh-free method. But because of the complexity of the integrand that results from the Petrov-Galerkin formulation, the integration difficulty is more severe than EFG. The MLPG method needs to be divided into small cells and more Gaussian quadrature points should be used for the integration [15]. The second reason for the increased processing time is that the system matrices produced by the MLPG method are asymmetric and those that are produced by the EFG methods are symmetric. The asymmetric matrices require more CPU time for their solution.

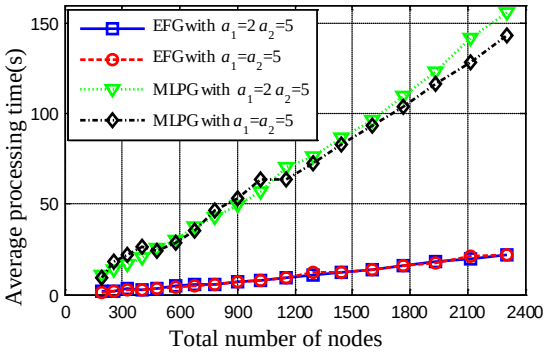

Fig. 12. Comparison of the proceeding time with different total number of nodes of EFG and MLPG method.

V. CONCLUSIONS

Implementations of the element free galerkin method (EFG) and the meshless local Petrov-Galerkin method have been presented in this paper. Both of the methods are formulated in detail for a basic problem governed by Poisson's equation. Problem domains governed by Poisson's and Helmholtz's equations have been considered and the numerical results are compared with the analytic solutions to investigate the accuracy and computational efficiency of the EFG method and the MLPG method. The results show that the MLPG method needs more CPU time but can obtain a more accurate result using fewer nodes than the EFG method. The reasons the MLPG method needs more processing time are that the MLPG method needs more integration points and

the solution of the asymmetric matrices require more CPU time.

ACKNOWLEDGMENT

This work is supported by the Major State Basic Research Development Program of China (973 Program) (No. 2011CB209401), the National Natural Science Foundation of China (Grant No. 51007096) and Scientific Research Foundation of State Key Lab. of Power Transmission Equipment and System Security (2007DA10512711203 &2007DA10512711102).

REFERENCES

[1] Q. Li and K. M. Lee, "An adaptive meshless method for magnetic field computation," *Magnetics, IEEE Transactions on*, vol. 42, pp. 1996-2003, 2006.

[2] G. R. Liu, *Meshfree Methods: Moving Beyond the Finite Element Method*, Boca Raton, CRC, 2009.

[3] T. Belytschko, Y. Y. Lu and L. Gu, "Element-free Galerkin methods," *International Journal for Numerical Methods in Engineering*, vol. 37, pp. 229-256, 1994.

[4] I. Singh, "Meshless EFG method in three-dimensional heat transfer problems: a numerical comparison, cost and error analysis," *Numerical Heat Transfer Part A: Applications*, vol. 46, pp. 199-220, 2004.

[5] M. H. Afshar, M. Naisipour and J. Amani, "Node moving adaptive refinement strategy for planar elasticity problems using discrete least squares meshless method," *Finite Elements in Analysis and Design*, vol. 47, pp. 1315-1325, 2011.

[6] P. F. Thomas and G. M. Hermann, "Classification and overview of meshfree methods," *Institute of Scientific Computing, Technical University Braunschweig*, Brunswick, Germany, 2004.

[7] R. D. Soares, R. C. Mesquita, F. J. S. Moreira, "Axisymmetric electromagnetic resonant cavity solution by a meshless local Galerkin method," *Applied Computational Electromagnetics Society (ACES) Journal*, vol. 26, pp. 792 – 799, 2011.

[8] R. K. Gordon, W. E. Hutchcraft, "The use of multiquadric radial basis functions in open region problems," *Applied Computational Electromagnetics Society (ACES) Journal*, vol. 21, pp. 127 – 134, 2006.

[9] K. Y. Dai, G. R. Liu, K. M. Lim, and Y. T. Gu, "Comparison between the radial point interpolation and the Kriging interpolation used in meshfree methods," *Computational Mechanics*, vol. 32, pp. 60-70, 2003.

[10] M. Fooladi, H. Golbakhshi, M. Mohammadi, and A. Soleimani, "An improved meshless method for analyzing the time dependent problems in solid mechanics," *Engineering Analysis with Boundary Elements*, vol. 35, pp. 1297-1302, 2011.

[11] S. N. Atluri and S. Shen, "The meshless local Petrov-Galerkin (MLPG) method: A simple & less-costly alternative to the finite element and boundary element methods," *CMES: Computer Modeling in Engineering & Sciences*, vol. 3, pp. 11-52, 2002.

[12] S. Ikuno, K. Takakura and A. Kamitani, "Influence of Method for Imposing Essential Boundary Condition on Meshless Galerkin/Petrov Galerkin Approaches," *Magnetics, IEEE Transactions on*, vol. 43, pp. 1501-1504, 2007.

[13] P. Lancaster and K. Salkauskas, "Surfaces generated by moving least squares methods," *Mathematics of Computation*, vol. 37, pp. 141-158, 1981.

[14] J. Dolbow and T. Belytschko, "An introduction to programming the meshless Element Free Galerkin method," *Archives of Computational Methods in Engineering*, vol. 5, pp. 207-241, 1998.

[15] S. N. Atluri, H. G. Kim and J. Y. Cho, "A critical assessment of the truly meshless local Petrov-Galerkin (MLPG), and local boundary integral equation (LBIE) methods," *Computational Mechanics*, vol. 24, pp. 348-372, 1999.

Wei He was born in 1957. He earned his Ph.D. in Germany in 1996. Now he is a Professor in school of electrical engineering, Chongqing University, China. His main research interests are in the areas of electromagnetic theory, electromagnetism environment and EMC and medical imaging.

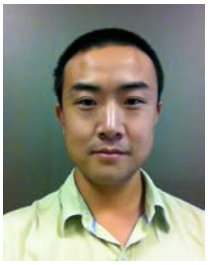

Zehui Liu was born in 1987, Henan Province, China. He got his B.S. in electrical engineering at Henan Polytechnic University at 2004. Now he is a Ph.D. candidate in the school of electrical engineering, Chongqing University, China. His research activities mainly include: electromagnetic environment of power system and meshless methods for solving electromagnetics problems.

Richard K. Gordon was born in Birmingham, Alabama on November 26, 1959. He earned his B.S. in physics at Birmingham Southern College, Birmingham, AL in 1983, his M.S. in mathematics at the University of Illinois, Urbana, IL in 1986 and his Ph. D. in electrical engineering at the University of Illinois, Urbana, IL in 1990. He is an Associate Professor in the Department of Electrical Engineering at the University of Mississippi in Oxford, Mississippi. Dr. Gordon is a member of Eta Kappa Nu, Phi Beta Kappa, and Tau Beta Pi.

W. Elliott Hutchcraft was born in Lexington, Kentucky on April 29, 1973. He earned his B.S. in electrical engineering at the University of Mississippi, Oxford, MS in 1996, and his M.S. in electrical engineering at the University of Mississippi, Oxford, MS in 1998 and his Ph. D. in electrical engineering at the University of Mississippi, Oxford, MS in 2003. He is an Associate Professor in the Department of Electrical Engineering at the University of Mississippi in Oxford, Mississippi. Dr. Hutchcraft is a member of Eta Kappa Nu, Sigma Xi, IEEE, Tau Beta Pi, Phi Kappa Phi, and ARFTG.

Fan Yang was born in ShanDong Province, China. Now he got his PhD degree in school of electrical engineering, Chongqing University, China and now he is an Associate Professor in electrical engineering of Chongqing University. His research of interests includes: high voltage electrical apparatus, electromagnetic devices and sensors, electromagnetic environment of power system.

Afei Chang was born in Anyang, Henan Province, China in 1986. She got her B.S. in electrical engineering at Henan Polytechnic University in 2004. She earned her M.S. in school of electrical engineering, Chongqing University, Chongqing, China. Now she is working in the State Nuclear Electric Power Planning Design & Research Institute, Beijing, China.